ORIGINAL ARTICLE

Mechanism of lncRNA SNHG19 miR-299-5p MAPK6 signaling axis promoting metastasis of non-small cell lung cancer cells

Qian Zhong , Rong Qiu (✉)

Department of Respiratory Medicine, Suining Central Hospital, Suining 629000, China

Abstract

Objective The aim of this study was to explore the mechanism behind lncRNA small nucleolar RNA host gene 19 (lncRNA SNHG19)/microrNA-299-5P (miR-299-5p)/mitogen-activated protein kinase 6 (MAPK6) signaling axis promoting metastasis of non-small cell lung cancer (NSCLC).

Methods To analyze the abnormal expression of lncRNAs in NSCLC, 50 surgically resected NSCLC and adjacent tissue samples were collected from August 2021 to August 2022. The mRNA expression levels of lncRNA SNHG19, Mir-299-5p, and MAPK6 were detected by qRT-PCR. The functions of lncRNA SNHG19, Mir-299-5p and MAPK6 were investigated by CCK-8, clone formation, EdU, scratch, Transwell western blotting (WB)and *in vivo* xenograft assay. RNA fluorescence *in-situ* hybridization (FISH), RNA pull-down, dual luciferase reporter, and RNA co-immunoprecipitation assays were used to explore the mechanism of action between lncRNA SNHG19, miR-299-5p, and MAPK6.

Results High expression of lncRNA SNHG19 was correlated with poor prognosis, tumor size, lymph node metastasis, and TNM stage in NSCLC patients ($P < 0.05$). Cell function experiments showed that lncRNA SNHG19 could improve the proliferation, clone formation, migration, and invasion ability of A549 cells both *in vitro* and *in vivo* (all $P < 0.05$) and increased the relative expression levels of vimentin and MAPK6 ($P < 0.05$). The relative expression level of E-cadherin was decreased ($P < 0.05$). lncRNA SNHG19 can interact with Mir-299-5p and regulate the expression level of MAPK6.

Conclusion lncRNA SNHG19 is upregulated in NSCLC tissues and cells, and its high expression is associated with tumor progression and poor survival. Moreover, it can act as a molecular sponge for Mir-299-5p to regulate MAPK6 expression and promote the proliferation and metastasis of A549 cells.

Key words: long noncoding RNA small nucleolar RNA host gene 19; MicroRNA-299-5p; non-small cell lung cancer (NSCLC); metastasis

The mortality and incidence of lung cancer rank among the top malignant tumors, and non-small cell lung cancer (NSCLC) patients have the worst prognosis [1]. At present, most treatment regimens are selected according to the stage of NSCLC as determined by the tumor, node and metastasis (TNM) classification of malignant tumors. However, due to the strong heterogeneity of NSCLC, there are great individual differences in treatment efficacy. It is difficult to meet the needs of clinical treatment when using only TNM classification as the basis for the selection of NSCLC treatment regimens. Therefore, it is necessary to further study the underlying molecular mechanisms related to the occurrence and development of NSCLC, to improve the early diagnosis and treatment

of NSCLC. Long non-coding RNA (lncRNA) is a class of transcripts with a length of more than 200 nucleotides. Several studies have shown that [2, 3], lncRNA is involved in various physiological and pathological processes such as cell differentiation, apoptosis, and migration. lncRNA small nucleolar RNA host gene 19 (SNHG19) is a recently discovered lncRNA, which has been confirmed to be abnormally expressed in the brain of pancreatic cancer [4], triple-negative breast cancer [5], other tumors, and Alzheimer's disease [6] patients. MicroRNA (miRNA) is a small non-coding RNA consisting of 19-25 nucleotides, which can affect the occurrence and development of tumors. Recent reports have shown that Mir-299-5p plays a cancer suppressor role in a variety of cancers [7]. The

results of a bioinformatics prediction using the ENCORI database showed that lncRNA SNHG19 had a target binding site for Mir-299-5p. Mitogen-activated protein kinase 6 (MAPK6) has a highly conserved gene sequence, which can activate cancer cell proliferation, survival, migration, and metastasis, and participate in angiogenesis and chemotherapy resistance through multiple signaling pathways, thus playing a cancer-promoting function [8]. In this study, the expression of lncRNA SNHG19, Mir-299-5p, and MAPK6 in NSCLC tissues and cell lines was detected, the changes in cell proliferation, migration, and invasion were observed, and the regulatory relationship between lncRNA SNHG19, Mir-299-5p and MAPK6 was analyzed. To explore the specific regulatory mechanisms of lncRNA SNHG19, Mir-299-5p, and MAPK6 in NSCLC, the following report is presented.

Materials and methods

Samples and participants

Samples from 50 patients having undergone surgical resection of NSCLC, from August 2021 to August 2022, were collected and confirmed as NSCLC by postoperative pathological diagnosis. All patients had complete clinical data and had not received radiotherapy or chemotherapy before operation. There were 26 males and 24 females, aged 55–73 (61.86 ± 5.14) years. At the same time, 50 cases of adjacent lung tissues were collected, which were pathologically diagnosed as normal lung tissues and frozen in liquid nitrogen. This study was approved by the ethics committee of our hospital (ethical approval number: 102467), and all patients gave informed consent and voluntarily provided tissue samples.

Reagents and instruments

Human bronchial epithelial cell line 16HBE and NSCLC cell lines A549, NCI-H292, NCI-H460, and NCI-H1703 were purchased from the Shanghai Cell Resource Center, Chinese Academy of Sciences. Dulbecco's modified eagle medium (DMEM) medium, fetal bovine serum, Streptomycin/penicillin, TRIzol reagent, High-capacity cDNA Reverse Transcription Kit, mirVana miRNA isolation Kit, Lipofectamine™ 2000 kit Streptomycin affinity coupled magnetic beads, and SuperSignal West Pico PLUS chemiluminescence substrate were purchased from Thermo Fisher (USA); construction, identification, packaging, and titer determination of lentiviral expression vectors were completed by Guangzhou Yuanjing Biotechnology Co., LTD, People's Republic of China. SYBR Premix Ex TAQii Kit was purchased from Dalian Baosheng Biotechnology Co., LTD, People's Republic of China. All-in-one miRNA qRT-PCR kit was purchased from Asia Pacific Hengxin Biotechnology (Beijing) Co., LTD, People's Republic of China. Polymerase chain reaction (PCR) primers and internal reference were purchased from Shanghai Shenggong Bioengineering Co., LTD, People's Republic of China. RNA fluorescence *in situ* hybridization (FISH) kit was purchased from Guangzhou Ruibo Biotechnology Co., LTD, People's Republic of China. Cck-8 kit, hematoxylin eosin (HE) staining and bicinchoninic acid (BCA) protein concentration assay kits were purchased from Shanghai Biyuntian Biotechnology Co., LTD, People's Republic of China. Matrigel matrix glue was purchased from Shanghai Yanhui Biotechnology Co., LTD, People's Republic of China. Rabbit Argonaute2 antibody, MAPK6, E-cadherin, vimentin, and Ki-67 were purchased from Abcam, Cambridge, UK. SP method rabbit antibody immunohistochemistry kit was purchased from Fuzhou Feijing Biotechnology Co., LTD, People's Republic of China. All other reagents were commercially available as analytically pure.

Cell culture, grouping and transfection

A549, NCI-H292, NCI-H460, NCI-H1703, and 16HBE cells were resuscitated and cultured with DMEM containing 10% fetal bovine serum and 100 mg/mL streptomycin/penicillin in an electric thermostatic incubator at 37°C, 5% CO_2, and saturated humidity. A549 was divided into the control group (without transfection), si-SNHG19 group (transfected si-SNHG19), SNHG19 group (transfected SNHG19), SNHG19-Mt group (transfected mutant SNHG19), miR-299-5p mimic group (transfected with miR-299-5p mimic), SNHG19+ miR-299-5p mimic group (transfected with SNHG19+ miR-299-5p mimic), si-SNHG19 + miR-299-5p inhibitor group (transfected with Si-SNHG19 + miR-299-5p inhibitor), si-MAPK6 group (transfected with SI-MAPK6), and SNHG19 + si-MAPK6 group (transfected with SNHG19+ si-MAPK6) and were transiently transfected according to the groups. The cells were collected 48 h post-transfection for subsequent experiments. A549 was divided into control group (without transfection), si-SNHG19 group (transfected si-SNHG19) and SNHG19 group (transfected SNHG19). Lentivirus transfection was performed according to the groups, and stable expression cell lines were constructed.

QRT-PCR of lncRNA SNHG19, miR-299-5p, and MAPK6 in tissues and cells

TRIzol reagent and mirVana miRNA isolation kit were used to extract total RNA and miRNAs from cancer tissues and cells of each group. Total RNA was transcribed into cDNA using a reverse transcription kit. A 20 μL PCR reaction mix was prepared using 1 μg cDNA template, 0.5 μg each of forward and reverse primers and SYBR Premix Ex TaQii kit. miRNAs were detected by all-in-one miRNA qRT-PCR kit. Reaction conditions: 94°C pre-denaturation for 2 min, 94°C for 30 s, 55°C for 30 s, 72°C

for 2 min for 35 cycles. qRT-PCR was performed using ABI 7500 real-time PCR instrument, and the relative expression levels of lncRNA SNHG19, miR-299-5p, and MAPK6 were calculated by the $2^{-\Delta\Delta CT}$ method.

FISH detection

FISH kit was used to detect the localization of lncRNA SNHG19 in A549 cells. Cells were routinely seeded on slides in 24-well plates, cultured for 24 h and then fixed with 4% paraformaldehyde for 10 min. We added 0.5% Triton X-100 and let it permeate for 5 min. The pre-hybridization solution and hybridization solution were preheated at 37°C for 30 min, then added to the slide and placed at 37°C for 20 min. The lncRNA SNHG19 probe was diluted at a ratio of 1:50 with hybridization solution, added to the slide, and kept away from light overnight at 37°C. The unbound probe was eluted, and 4', 6-diamidino-2-phenylindole (DAPI) was added to avoid light reaction for 8 min. The anti-fluorescence quench was dropped, and the slices were sealed, observed, and photographed under the BX51 fluorescence microscope (Olympus Company of Japan) was used.

RNA pull-down test

A549 cells were taken and transfected with biotin-labeled Mir-299-5p. After 48 h of normal culture, appropriate lysates were added to fully lysate the cells. The lysates were collected, streptomycin affinity coupled magnetic beads were added, fully mixed, and incubated at 4°C for 3 h. lncRNA SNHG19 levels were detected by qRT-PCR.

Dual luciferase reporter assay

The wild-type psicheck2-SnHG19-Luc and mutant PsichecK2-SnHG19-Mut-Luc fluorescent plasmids were constructed and co-transfected into A549 cells with Mir-299-5p mimics. The wild-type PsichecK2-MAPK6-Luc fluorescent plasmid was constructed. The cells were transfected into the control group, Si-SNHG19 group, SI-SNHG19 + Mir-299-5p inhibitor group, SNHG19 group, SNHG19-MT group, and SNHG19+ Mir-299-5p mimic group, and the luciferase activity in each group was detected by Varioskan LUX enzyme labeling instrument (Thermo Fisher Company of USA).

RNA immunoprecipitation

A549 cells were harvested and lysed with an appropriate amount of lysate. AGO2 antibody and immunoglobulin G (IgG) were added to the magnetic beads, incubated at room temperature (20–25°C) for 30 min, then cell lysates were added, incubated overnight at 4°C, and purified immunoprecipitated RNA was detected by qRT-PCR.

CCK-8 assay

Cells in the logarithmic growth phase were inoculated in 96-well plates after trypsin digestion and cultured for 5 d. Cck-8 was detected once a day. Cck-8 solution was added to each well and the culture was continued for 2 h.

Determination of cell proliferation ability

Clone formation experiment: after trypsin digestion, the cells in each group were seeded in a 6-well plate at an inoculation density of 1000 cells/well. The cells were cultured in a 5% CO_2 incubator at 37°C for 10 d. The medium was discarded, washed with $1 \times$ PBS, fixed with methanol for 30 min, and stained with 1% crystal violet for 20 min. Then we observed, photographed, and clone counted.

BrdU incorporation experiment: Cells were seeded in 24-well plates with 3×10^5 cells per well, fixed with 4% paraformaldehyde for 20 min, washed 3 times with PBS, underwent DNA proteolysis for 30 min, incubated in 0.2% Triton X-100 for 8 min, washed 3 times with PBS, and blocked with 10% fetal bovine serum for 1 h. The cells were incubated with primary antibody against BrdU (1:1000), washed with PBS, and incubated with secondary antibody against light for 1 h. BrdU positive cells were observed and counted under a fluorescence microscope.

Scratch test

The cells in the logarithmic growth phase of each group were seeded in 6-well plates at a cell density of 1×10^6 cells/well, and the cell confluency was observed to reach 90%. Scratches were made with a 200 μL pipette tip to remove the shed cells, and serum-free medium was added and cultured for 24 h. Photos were taken immediately after the scratch and then again after 24 h of culturing, and the scratch width was measured using Image J software (National Institutes of Health.). The cell migration rate was calculated as: (initial scratch width − scratch width after 24 h)/initial scratch width ×100%.

Transwell experiment

Serum-free DMEM medium was diluted with Matrigel glue at a ratio of 1:3, and evenly spread on the bottom of the upper chamber membrane after mixing. The medium was placed overnight in a 37°C incubator with 5% CO_2 and exposed to ultraviolet light for 30 min the next day. Cells passing through the upper chamber were fixed with 4% paraformaldehyde for 30 min, stained with crystal violet, observed, and photographed under a light microscope, and the cell invasion rate was calculated as the number of invaded cells in each group/the number of invaded cells in the control group × 100%.

Western blotting

Samples of NSCLC and adjacent tissues were homogenized, and an appropriate amount of pre-cooled radio immunoprecipitation assay (RIPA) was added, and the mixture was fully mixed and incubated for 1.5 h on ice. After centrifugation at 20,000 g at 4°C for 10 min, the supernatant was removed, and the sample was prepared after BCA quantification. The protein of the sample was separated by gel electrophoresis, the membrane was turned, and the target band was intercepted and immersed in the blocking solution made of 5% skim milk powder, and then blocked on a shaker for 1 h at room temperature. The blocking solution was diluted to make the incubation solution, with a dilution ratio of 1:500, and the solution was fully shaken and left to incubate overnight at 4°C. After washing the film, the corresponding secondary antibody incubation solution with a dilution ratio of 1:5000 was added and incubated at room temperature for 2 h. Electrochemiluminescence solution (ECL) chemiluminescence solution was added and the reaction was kept away from light for 5 min. The results were collected using quantitative imager.

In vivo xenograft experiments

Nude mice were randomly divided into 16 groups according to the cell name of each group. Eight cells were randomly divided into each group and injected into both sides of the axilla with a density of 5×10^6 cells / ml. The volume of subcutaneous tumors was measured every 4 d with a digital caliper, and the formula was: volume =1/2 (length × width^2). After 23 d, the nude mice were euthanized, and the tumors were completely removed. The tumors were measured and photographed, fixed in 10% formaldehyde solution, and then embedded in paraffin and sectioned. The remaining 8 mice were injected with cell suspension at a density of 3×10^6 cells /mL through the tail vein. After 60 d, the nude mice were euthanized, and the lung tissues were completely removed and photographed as paraffin sections.

HE staining was used to observe metastatic lung nodules of NSCLC

Paraffin sections were stained according to the instructions of the HE staining kit, observed and photographed under a light microscope, and the number of lung nodules was calculated.

Immunohistochemical analyses

Immunohistochemical streptavidin-perosidase (SP) method was used to detect the expression of MAPK6 in NSCLC and adjacent tissues and Ki-67, E-cadherin, and vimentin in nude mouse tumors. The paraffin sections were processed and stained according to the

kit requirements, and the experimental results were photographed under the light microscope. Five different fields were randomly selected for each section, and Image J software was used for image analysis. The average value was taken as the relative expression levels of Ki-67, E-cadherin, and vimentin.

Statistical analysis

SPSS 24.0 (Chicago, IL, USA) statistical software was used to analyze and process the data. Measurement data were expressed as mean ± standard deviation ($\chi \pm s$). Independent sample t-test was used for the comparison between two groups, and one-way analysis of variance was used for the comparison between multiple groups. Enumeration data were expressed in the form of rate (%), and comparison between groups was performed by chi-square test. $P < 0.05$ indicates statistical significance.
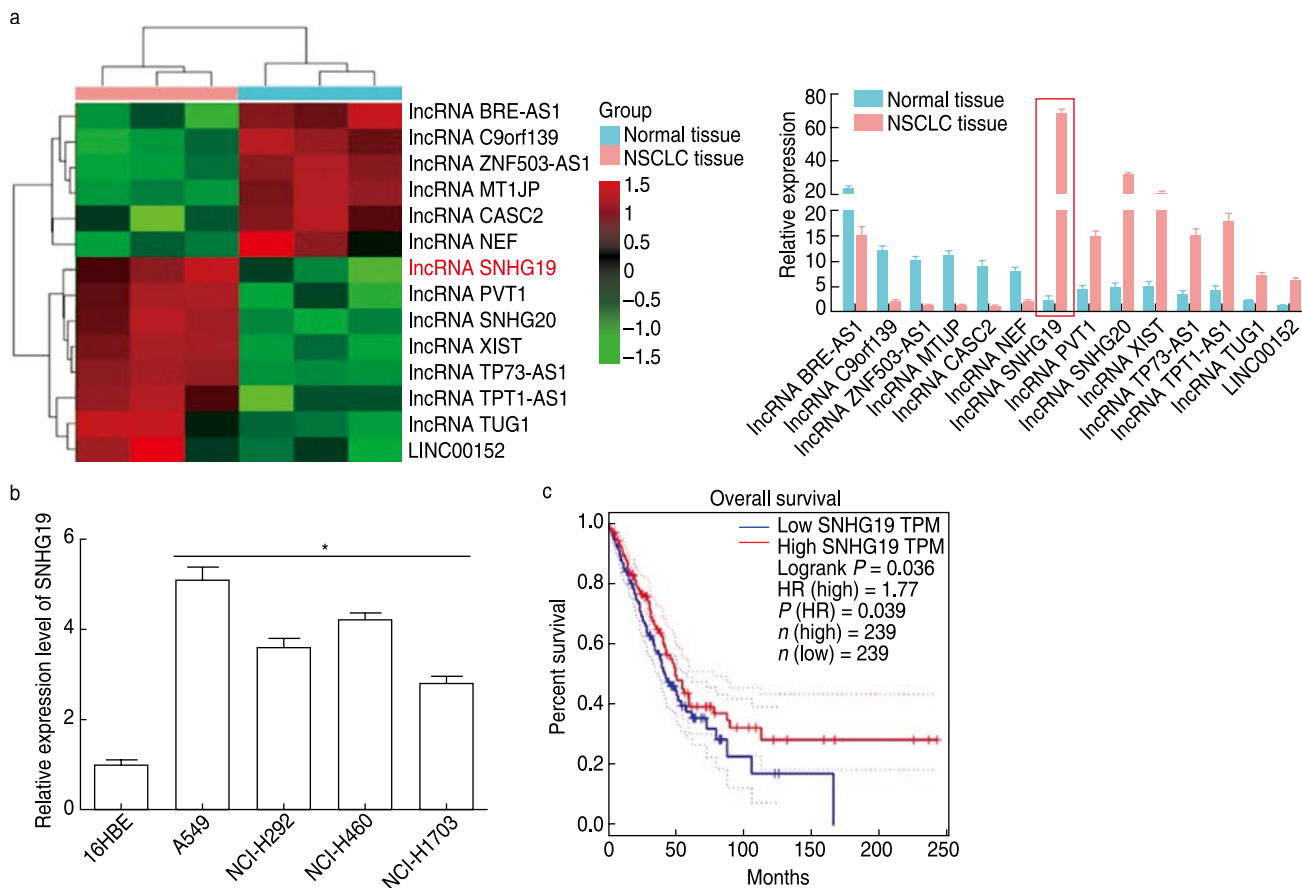
Results

The relationship between lncRNA SNHG19 expression and clinicopathological features in NSCLC

Among the multiple aberrantly expressed lncRNAs in NSCLC, lncRNA SNHG19 is one of the significantly upregulated lncRNAs with high relative abundance (Fig. 1a). The results of qRT-PCR detection showed (Fig. 1b) that the relative expression of lncRNA SNHG19 was increased in NSCLC cell lines ($P < 0.05$). The relative expression of lncRNA SNHG19 was the highest in A549 cells, therefore A549 cells were selected for subsequent experiments. The results of survival analysis showed (Fig. 1c) that high expression of lncRNA SNHG19 was significantly associated with overall survival ($P < 0.05$). The expression of lncRNA SNHG19 was correlated with tumor size, lymph node metastasis, and TNM classification in patients with NSCLC ($P < 0.05$) (Table 1).

lncRNA SNHG19 promotes the growth of NSCLC cells in vitro

The results of CCK-8 (Fig. 2a), colony formation (Fig. 2b), scratch (Fig. 2c), and Transwell experiments (Fig. 2d) showed that compared with the control group, the si-SNHG19 group had better proliferation, colony formation, migration, and invasion abilities. These abilities of the SNHG19 group were significantly improved, and the difference with the control group was statistically significant ($P < 0.05$). The results of WB detection showed that (Fig. 2e), compared with the expression levels of E-cadherin and vimentin in the control group, the relative expression level of E-cadherin increased and the relative expression level of vimentin decreased in the

Fig. 1 Expression of lncRNA SNHG19 in NSCLC. (a) Hierarchical clustering heatmap of aberrantly expressed lncRNAs in NSCLC; (b) Tissue qRT-PCR test results; (c) qRT-PCR detection results of NSCLC cell lines; (d) Survival analysis results

si-SNHG19 group, while the relative expression level of E-cadherin decreased and the relative expression level of vimentin increased in the SNHG19 group. The difference was statistically significant ($P < 0.05$).

lncRNA SNHG19 promotes proliferation and metastasis of NSCLC cells in vivo

The results of the *in vivo* xenograft experiments showed that the tumor volume for the si-SNHG19 group was smaller than that for control group, and the tumor volume for the SNHG19 group was bigger than that for control group ($P < 0.05$, Fig. 3a). The results of qRT-PCR detection (Fig. 3b) showed that compared with the expression of lncRNA SNHG19 in the control group, the expression of lncRNA SNHG19 in the si-SNHG19 group decreased, while the expression of lncRNA SNHG19 in the SNHG19 group increased ($P < 0.05$), suggesting that the recombinant vectors were stably expressed in each group. The results of lung tissue HE staining (Fig. 3c) showed that compared with the nodules in the control group, the number of metastatic lung nodules in the si-SNHG19 group decreased, and the number of metastatic lung nodules in the SNHG19 group increased ($P < 0.05$).

The results of immunohistochemistry showed (Fig. 3d) that compared with the control group, the relative expression levels of Ki-67 and vimentin in the si-SNHG19 group decreased, while those of E-cadherin increased, and the relative expression levels of Ki-67 and vimentin in the SNHG19 group increased while those of E-cadherin decreased ($P < 0.05$).

lncRNA SNHG19 regulates the expression of miR-299-5p in NSCLC

qRT-PCR detection results showed (Fig. 4a) that miR-299-5p was lowly expressed in NSCLC tissues and cell lines ($P < 0.05$). After fluorescent staining, lncRNA SNHG19 was red, the nucleus was blue, and lncRNA SNHG19 was mainly expressed in the cytoplasm (Fig. 4b). RNA pull-down assay and dual-luciferase reporter gene assay showed (Fig. 4c) that miR-299-5p could be pulled down by lncRNA SNHG19, and miR-299-5p mimic could reduce lncRNA SNHG19 luciferase of wild-type 3'UTR. The lncRNA SNHG19 luciferase activity had no effect on the mutant 3'UTR lncRNA SNHG19, indicating that lncRNA SNHG19 can directly target miR-299-5p. The results of co-immunoprecipitation assay (Fig. 4d) showed

Table 1   Relationship between lncRNA SNHG19 expression and clinicopathological features of NSCLC patients [n (%)]

Pathological features	n	lncRNA SNHG19		χ^2 value	P value
		High expression	Low expression		
Age (years)				0.321	0.571
≤ 49	26	12 (48.00)	14 (56.00)		
> 49	24	13 (52.00)	11 (44.00)		
Sex				1.282	0.258
Male	26	11 (44.00)	15 (60.00)		
Female	24	14 (56.00)	10 (40.00)		
Smoking history				1.282	0.258
No	24	10 (40.00)	14 (56.00)		
Yes	26	15 (60.00)	11 (44.00)		
Histological type				1.064	0.786
Adenocarcinoma	26	14 (56.00)	12 (48.00)		
Squamous cell carcinoma	13	6 (24.00)	7 (28.00)		
Adenosquamous carcinoma	8	3 (12.00)	5 (20.00)		
Large-cell carcinoma	3	2 (8.00)	1 (4.00)		
Tumor size (cm)				12.500	< 0.001
≤ 3	18	15 (60.00)	3 (12.00)		
> 3	32	10 (40.00)	22 (88.00)		
Tumor differentiation				0.347	0.556
High-middle grade	32	15 (60.00)	17 (68.00)		
Low grade	18	10 (40.00)	8 (32.00)		
Lymph node metastasis				5.195	0.023
No	28	18 (72.00)	10 (40.00)		
Yes	22	7 (28.00)	15 (60.00)		
TNM classification (stage)				4.160	0.041
I–II		19 (76.00)	12 (48.00)		
III		6 (24.00)	13 (52.00)		

that both lncRNA SNHG19 and miR-299-5p were significantly enriched in the microriboprotein complex of AGO2, indicating that AGO2 protein directly binds to lncRNA SNHG19 and miR-299-5p in NSCLC cells. The results of CCK-8 (Fig. 4e), EdU (Fig. 4f), and Transwell experiments (Fig. 4g) showed that compared with the proliferation and migration abilities of the control group, those of the SNHG19+miR-299-5p mimic group had no significant difference (P > 0.05), those of the SNHG19 group were significantly improved, while those of the miR-299-5p mimic group were significantly decreased (P < 0.05).

lncRNA SNHG19 affects the expression of MAPK6 in NSCLC by regulating miR-299-5p

The results of qRT-PCR showed (Fig. 5a) that the expression of MAPK6 was significantly upregulated in NSCLC tissues and cell lines (P < 0.05). The results of WB detection showed (Fig. 5b) that compared with MAPK6 expression level of the control group, the relative expression level of MAPK6 was significantly decreased, and increased in the si-SNHG19 and SNHG19 groups, respectively (P < 0.05). The relative expression level of MAPK6 was significantly increased and decreased

in the +miR-299-5p inhibitor SNHG19+miR-299-5p mimic groups, respectively (P < 0.05). The results of dual-luciferase reporter gene detection showed (Fig. 5c) that the fluorescence of Luc-MAPK6 in the SNHG19-Mt group, si-SNHG19+miR-299-5p inhibitor group, and SNHG19+miR-299-5p mimic group was significantly higher than that in the control group. There was no significant difference in luciferase activity (P > 0.05). The activity of Luc-MAPK6 luciferase was significantly decreased and increased in the si-SNHG19 SNHG19 groups, respectively (P < 0.05). The results of the co-immunoprecipitation assay showed (Fig. 5d) that the enrichment of AGO2 on SNHG19 decreased and the enrichment on MAPK6 increased after silencing lncRNA SNHG19, while the enrichment of AGO2 on SNHG19 in cells overexpressing lncRNA SNHG19 increased, and the enrichment on MAPK6 decreased (P < 0.05).

**The cancer-promoting effect of lncRNA SNHG19 is associated with MAPK6**

The results of CCK-8 (Fig. 6a), EdU (Fig. 6b), and Transwell experiments (Fig. 6c) showed that compared with the proliferation and migration abilities of cells control group, those in the SNHG19 group were
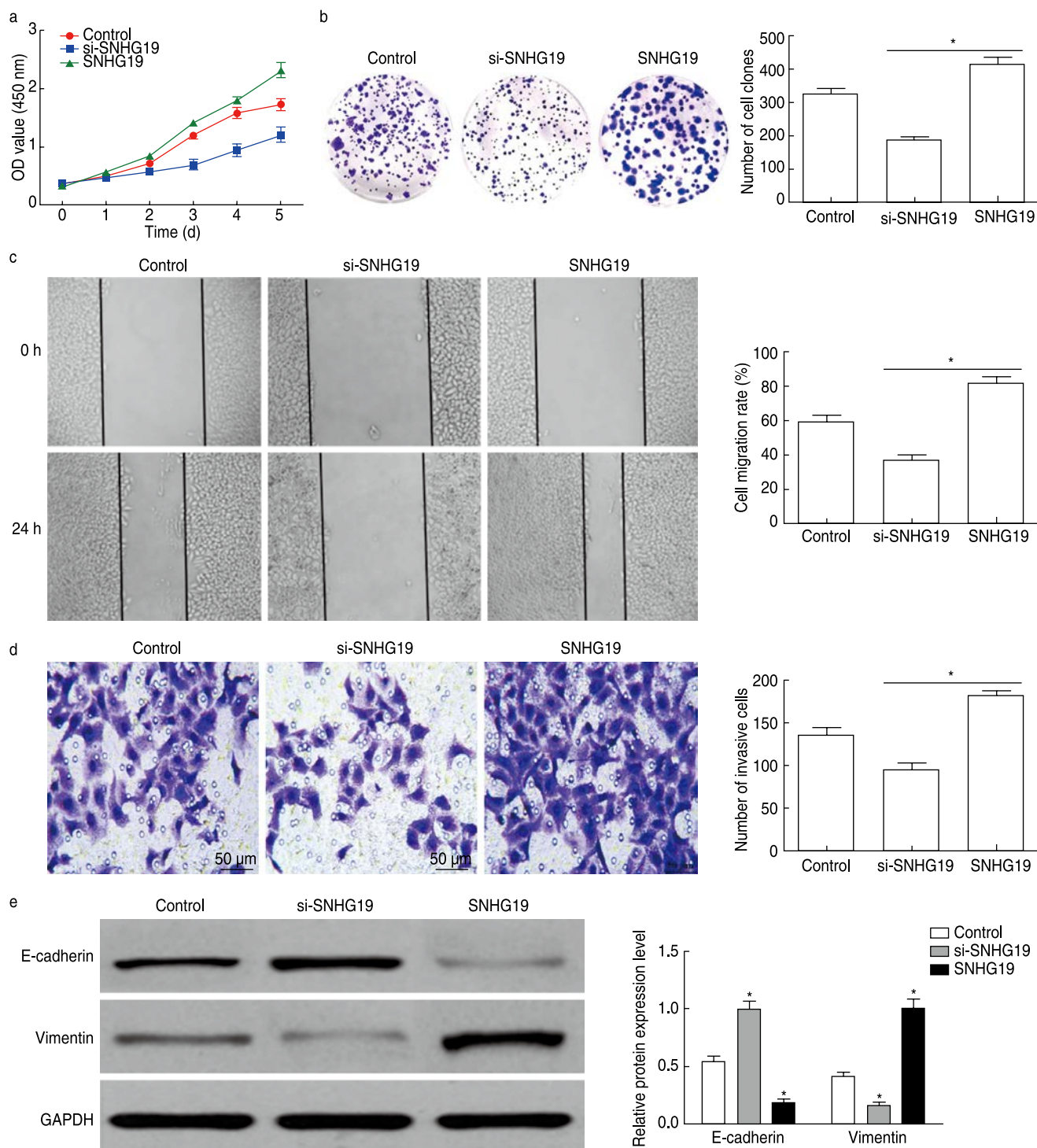
Fig. 2   lncRNA SNHG19 promotes NSCLC cell growth *in vitro*. (a) CCK-8 test results; (b) Experimental results of clone formation; (c) Scratch test results; (d) Transwell experimental results; (e) Western blotting test results. Compared with the control group, * P < 0.05

significantly improved, while those of the cells in the si-MAPK6 group were significantly reduced (*P* < 0.05). The results of WB detection showed (Fig. 6d) that compared with the control group, the relative expression levels of E-cadherin in the si-SNHG19 group and si-MAPK6 group

were significantly increased, and the relative expression levels of vimentin and MAPK6 were significantly decreased. The relative expression levels of E-cadherin in the SNHG19 group were significantly decreased, while the relative expression levels of vimentin and MAPK6
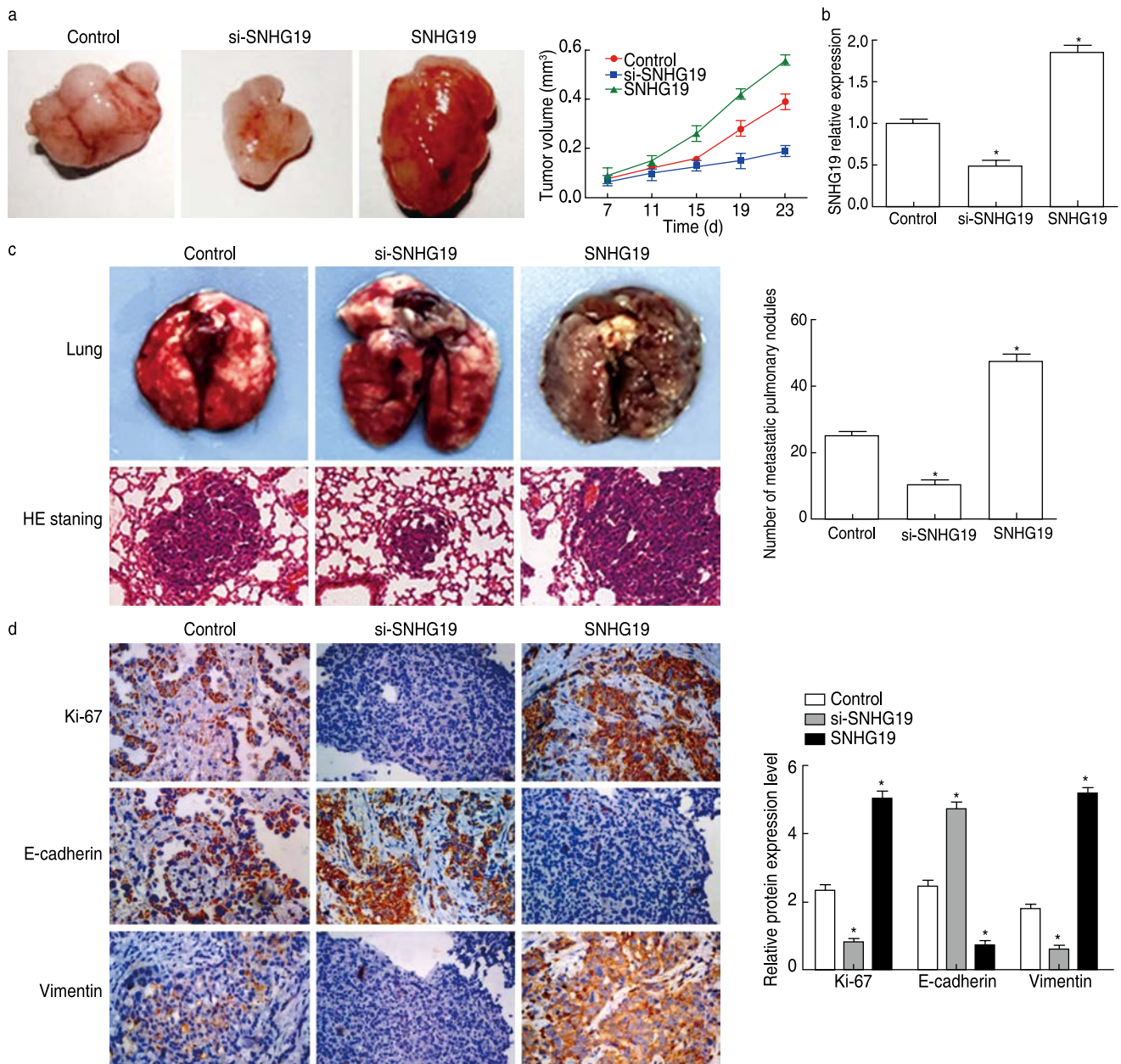
Fig. 3   lncRNA SNHG19 promotes proliferation and metastasis of NSCLC cells *in vivo*. (a) Results of *in vivo* xenograft experiments; (b) qRT-PCR test results; (c) HE staining results and quantitative observation of metastatic pulmonary nodules; (d) Immunohistochemical test results (× 400). Compared with the control group, * $P < 0.05$

were significantly increased ($P < 0.05$).

The mechanism of lncRNA SNHG19 affecting NSCLC by regulating MAPK6 through miR-299-5p

The results of this study showed that lncRNA SNHG19 and MAPK6 were upregulated in NSCLC and played a tumor-promoting role, while miR-299-5p was down-regulated and played a tumor suppressor role. There is a targeted inhibitory relationship between MAPK6, and

it is speculated that lncRNA SNHG19 regulates MAPK6 through miR-299-5p, and its possible mechanism is shown in Fig. 7.

Discussion

In the human genome, in addition to miRNAs with powerful regulatory and epigenetic modification functions, there are many other noncoding RNAs. lncRNAs were initially considered to be by-products
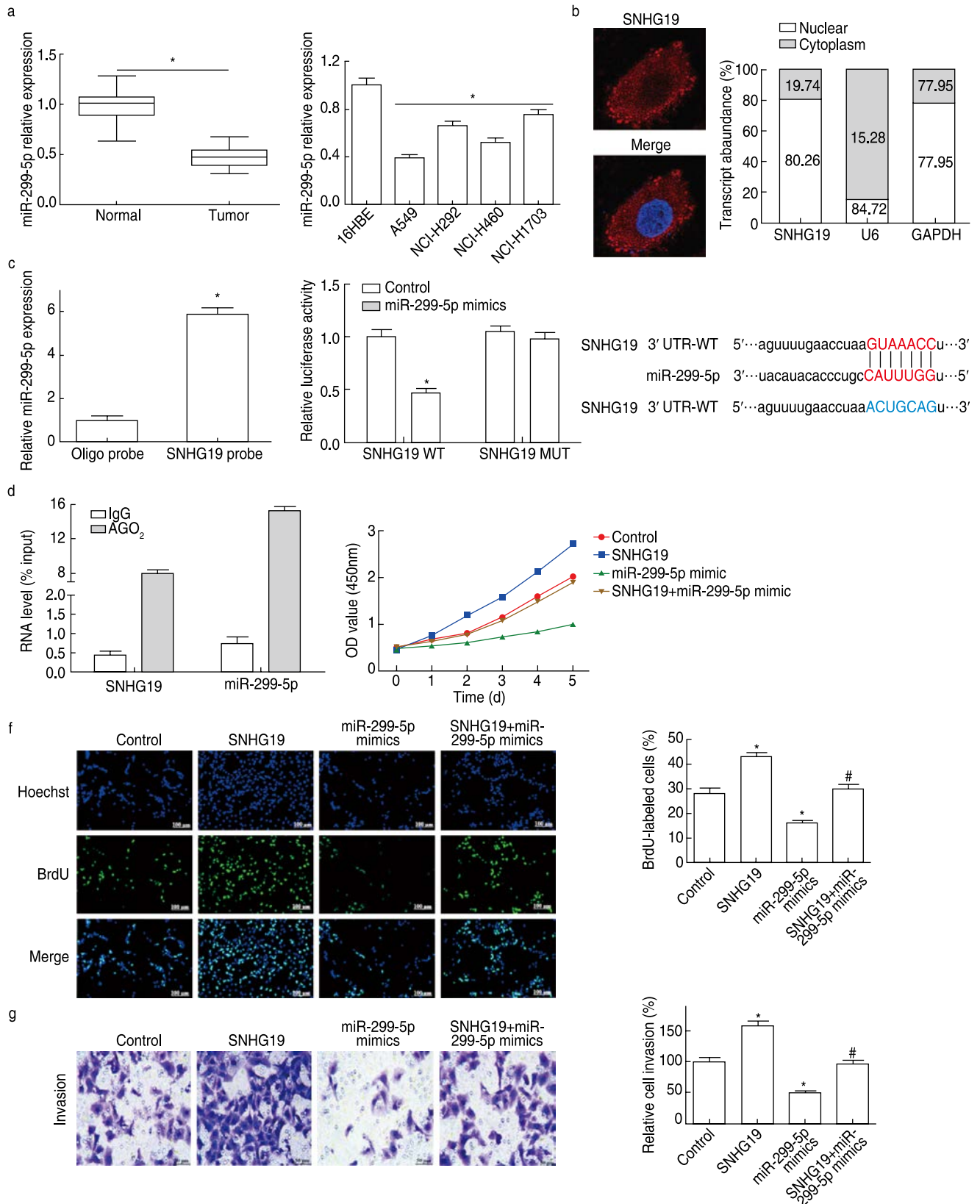
Fig. 4 lncRNA SNHG19 regulates the expression of miR-299-5p in NSCLC. (a) qRT-PCR test results; (b) FISH test results; (c) RNA pull-down assay and dual-luciferase reporter gene assay results; (d) Co-immunoprecipitation test results; (e) CCK-8 test results; (f) EdU test results; (g) Transwell test results. Compared with the control group, *P < 0.05; compared with the SNHG19 group, #P < 0.05
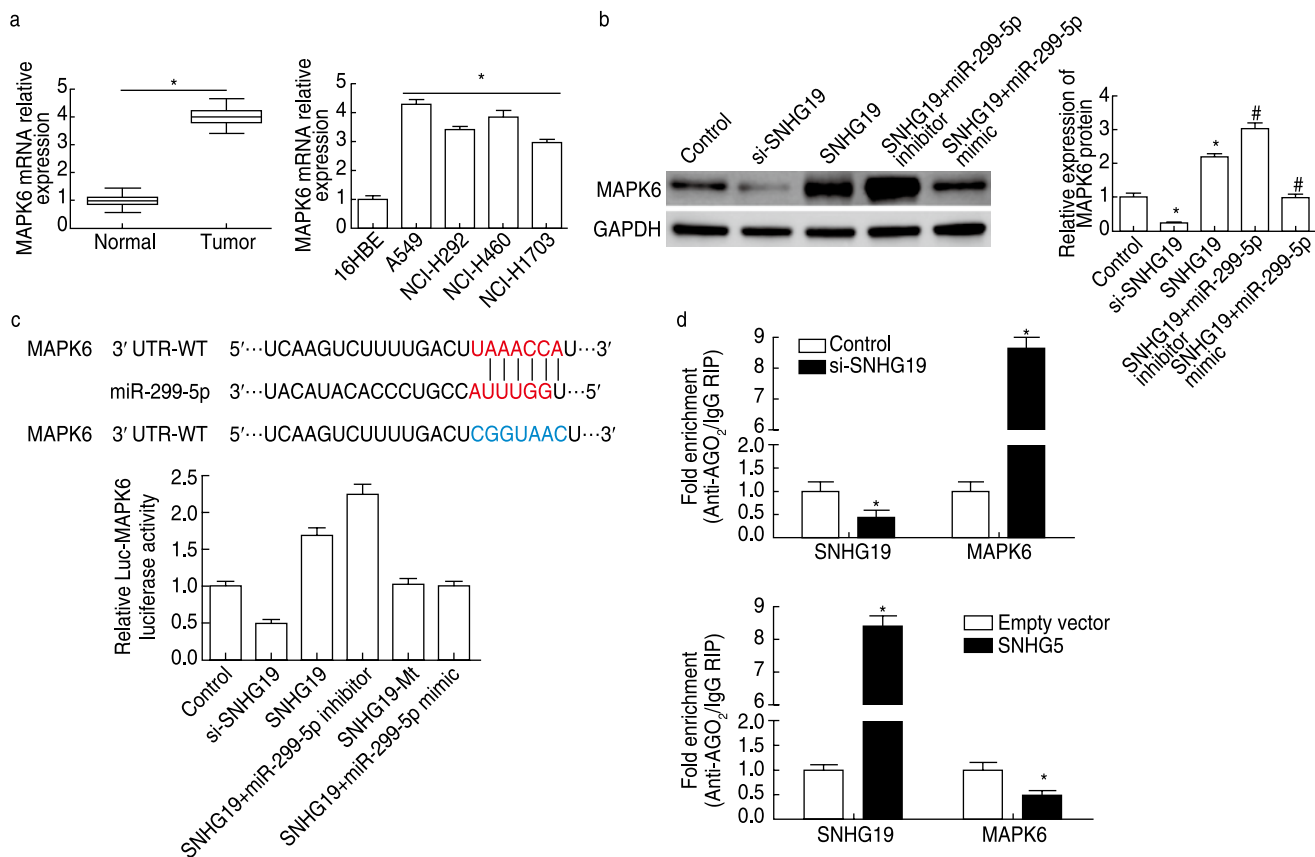
Fig. 5 lncRNA SNHG19 affects the expression of MAPK6 in NSCLC by regulating miR-299-5p. (a) qRT-PCR test results; (b) Western blotting test results; (c) Dual-luciferase reporter gene assay results; (d) Co-immunoprecipitation test results. Compared with the control group, * P < 0.05; compared with the SNHG19 group, # P < 0.05

of RNA polymerase II transcription and genomic noise, however, increasing evidence suggests that they can participate in many biological processes and play an important role in the occurrence and development of diseases [9, 10]. Wu [11] found that lncRNA DUXAP8 can promote the proliferation, epithelial-mesenchymal transition (EMT) and aerobic glycolysis of NSCLC cells, and its high expression is related to the poor prognosis of NSCLC patients. The study of Zeng [12] showed that lncRNA PVT1 is upregulated in NSCLC tissues and cell lines, which can promote the proliferation, migration, and invasion of NSCLC cells. The study of Wang [13] confirmed that the expression of lncRNA HNF1A-AS1 is upregulated in NSCLC tissues and cells, which can promote cell proliferation and inhibit cell apoptosis, and is closely related to the clinicopathological stage of patients. Knockout of lncRNA HNF1A-AS1 can significantly enhance the radiosensitivity of NSCLC cells. These studies prove that in-depth understanding of the role of lncRNA in NSCLC is beneficial for improved diagnosis and treatment efficiency of NSCLC.

lncRNA SNHG19 was first discovered in Alzheimer's disease brain tissue [6]. Subsequent studies have shown [5]

that it is highly expressed in breast cancer tissues. The results of Zhao [14] showed that lncRNA SNHG19 was upregulated in NSCLC cancer tissues, cell lines, and patient plasma, and could promote the proliferation, migration, and invasion of NSCLC cells. However, a few studies have reported on the relationship between the expression of lncRNA SNHG19 and the occurrence and development of NSCLC, and its energy supply in NSCLC has not been fully elucidated. In this study, lncRNA SNHG19 was abnormally expressed in NSCLC tissues and cell lines, and its high expression indicated that the patient's NSCLC was in the advanced stage and had a poor prognosis. Cell function experiments in this study showed that lncRNA SNHG19 could significantly promote the proliferation and metastasis of NSCLC both *in vitro* and *in vivo*. The results from a bioinformatics prediction using ENCOPI database showed that lncRNA SNHG19 has a binding site with miR-299-5p, but no studies have confirmed the targeting effect of the two. In order to explore the mechanism of lncRNA SNHG19 in NSCLC, this study confirmed that lncRNA SNHG19 can act as a molecular sponge for miR-299-5p in the cytoplasm and exert its cancer-promoting effect by regulating the level of MAPK6. We used RNA
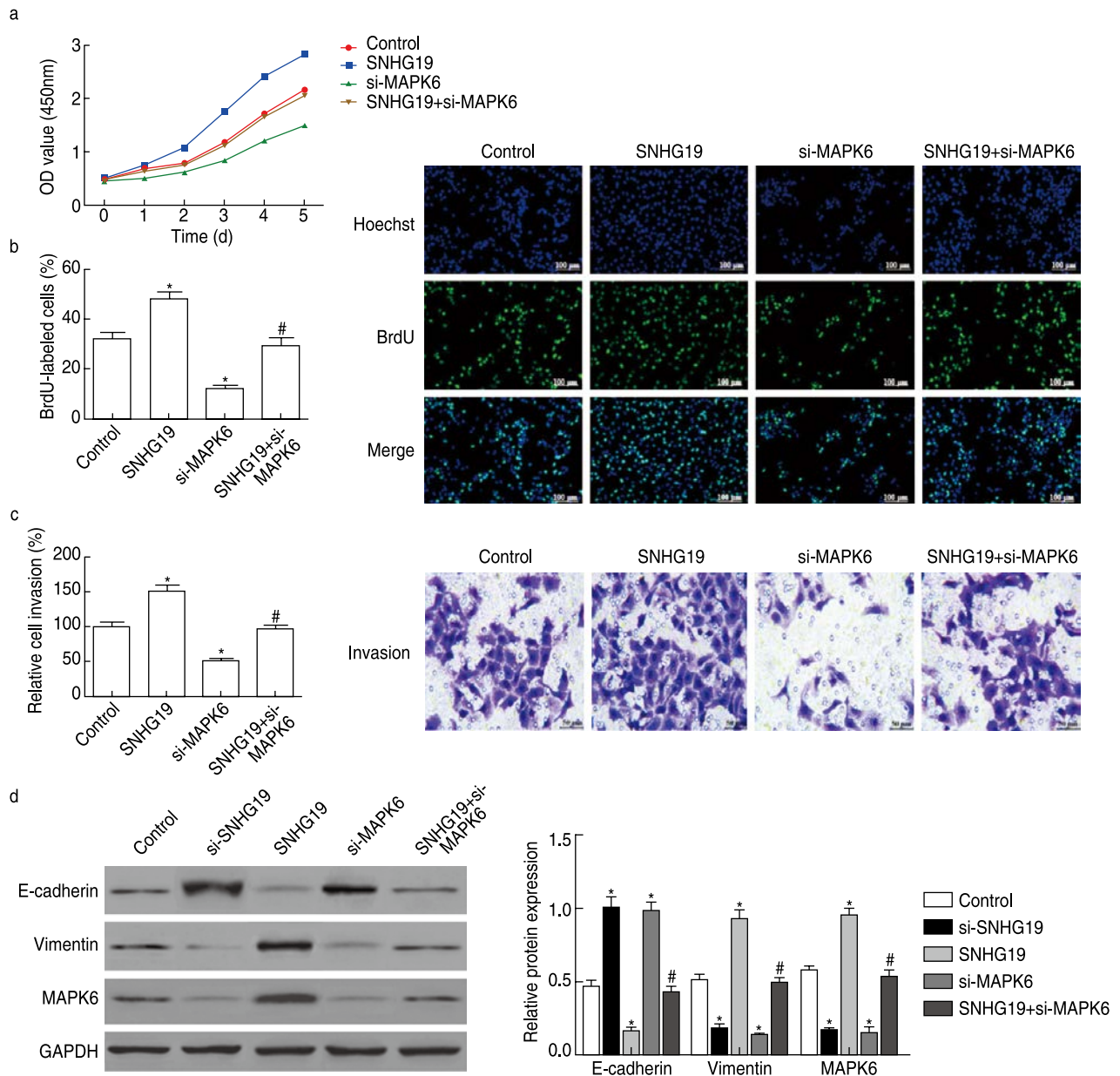
Fig. 6 The cancer-promoting effect of lncRNA SNHG19 is associated with MAPK6. (a) CCK-8 test results; (b) EdU test results; (c) Transwell experimental results; (d) Western blotting test results. Compared with the control group, * $P < 0.05$; compared with the SNHG19 group, # $P < 0.05$
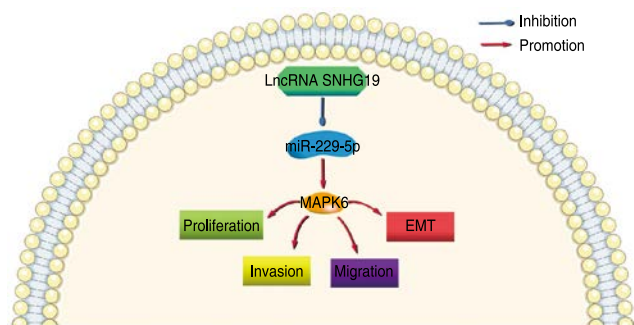
Fig. 7 Illustration of the mechanism of lncRNA SNHG19 affecting NSCLC by regulating MAPK6 through miR-299-5p

pull-down assay, dual-luciferase reporter gene detection, and RNA co-immunoprecipitation detection to reach these results. A potential site for miR-299-5p binding in the MAPK6 3'UTR was also shown in the Target Scan Human database. However, a few studies report on the specific mechanism of lncRNA SNHG19/miR-299-5p/ MAPK6 signaling axis in NSCLC.

MAPK6, also known as ERK3, is an atypical member of the MAPK family, which is associated with the metastasis of breast and gastric cancers and is an important molecule in the occurrence and development of cancer in general[15, 16]. The results of Wu[17] showed that MAPK6 is upregulated

in NSCLC cells and is involved in the occurrence and development of NSCLC under the regulation of hsa-miR-98-5p and lncRNA NEAT1. Epithelial-mesenchymal transition is a key process in cancer cell metastasis, during which epithelial cells lose their ability to adhere to cells and acquire a variety of mesenchymal properties including invasion and migration. The upregulated and downregulated levels of the mesenchymal cell marker vimentin and epithelial marker E-cadherin, respectively, are characteristic of EMT. MAPK6 levels are closely related to EMT [18]. The research report of Lv [19] showed that MAPK6 can activate the EMT process, thereby promoting the proliferation, migration and invasion of breast cancer cells, which is closely related to the prognosis of breast cancer patients. In this study, silencing lncRNA SNHG19 down-regulated the expression level of MAPK6 and suppressed the expression of EMT-related proteins, suggesting that MAPK6 is involved in the carcinogenesis of lncRNA SNHG19 in NSCLC.

In conclusion, lncRNA SNHG19 is upregulated in NSCLC tissues and cells, and its high expression is associated with tumor progression and poor survival. lncRNA SNHG19 acts as a molecular sponge for miR-299-5p to regulate MAPK6 expression and promote the proliferation and metastasis of A549 cells, which may become a new biomarker and therapeutic target for NSCLC.

Conflicts of interest

The authors indicated no potential conflicts of interest.

Author contributions

Not applicable.

Data availability statement

Not applicable.

Ethical approval

Not applicable.

References

1. Luo Y, Ma S, Sun Y, et al. MUC3A induces PD-L1 and reduces tyrosine kinase inhibitors effects in EGFR-mutant non-small cell lung cancer. Int J Biol Sci. 2021;17(7):1671-1681.
2. Rakhshan A, Esmaeili MH, Kahaei MS, et al. A Single Nucleotide Polymorphism in GAS5 lncRNA is Associated with Risk of Bladder Cancer in Iranian Population. Pathol Oncol Res. 2020;26(2):1251-1254.
3. Wu D, Li H, Wang J, et al. LncRNA NEAT1 promotes gastric cancer progression via miR-1294/AKT1 axis. Open Med (Wars). 2020;15(1):1028-1038.
4. Chang YW, Hsu CL, Tang CW, et al. Multiomics reveals ectopic ATP synthase blockade induces cancer cell death via a lncRNA-mediated Phospho-signaling network. Mol Cell Proteomics. 2020;19(11):1805-1825.
5. Li XX, Wang LJ, Hou J, et al. Identification of long noncoding RNAs as predictors of survival in triple-negative breast cancer based on network analysis. Biomed Res Int. 2020;2020:8970340.
6. Cao M, Li H, Zhao J, et al. Identification of age- and gender-associated long noncoding RNAs in the human brain with Alzheimer's disease. Neurobiol Aging. 2019;81:116-126.
7. Fateh A, Feizi MAH, Safaralizadeh R, et al. Importance of miR-299-5p in colorectal cancer. Ann Gastroenterol. 2017;30(3):322-326.
8. Elkhadragy L, Alsaran H, Long W. The C-Terminus Tail regulates ERK3 kinase activity and its ability in promoting cancer cell migration and invasion. Int J Mol Sci. 2020;21(11):4044.
9. Chen X, Yang Y, Sun J, et al. LncRNA HCG11 represses ovarian cancer cell growth via AKT signaling pathway. J Obstet Gynaecol Res. 2022;48(3):796-805.
10. Xu G, Yang H, Liu M, et al. lncRNA TINCR facilities bladder cancer progression via regulating miR 7 and mTOR. Mol Med Rep. 2020;22(5):4243-4253.
11. Wu C, Song W, Wang Z, et al. Functions of lncRNA DUXAP8 in non-small cell lung cancer. Mol Biol Rep. 2022;49(3):2531-2542.
12. Zeng SHG, Xie JH, Zeng QY, et al. lncRNA PVT1 promotes metastasis of non-small cell lung cancer through EZH2-mediated activation of Hippo/NOTCH1 signaling pathways. Cell J. 2021;23(1):21-31.
13. Wang Z, Liu L, Du Y, et al. The HNF1A-AS1/miR-92a-3p axis affects the radiosensitivity of non-small cell lung cancer by competitively regulating the JNK pathway. Cell Biol Toxicol. 2021;37(5):715-729.
14. Zhao GY, Ning ZF, Wang R. LncRNA SNHG19 promotes the development of non-small cell lung cancer via mediating miR-137/E2F7 Axis. Front Oncol. 2021;11:630241.
15. Cai Q, Zhou W, Wang W, et al. MAPK6-AKT signaling promotes tumor growth and resistance to mTOR kinase blockade. Sci Adv, 2021;7(46):eabi6439.
16. Bogucka K, Pompaiah M, Marini F, et al. ERK3/MAPK6 controls IL-8 production and chemotaxis. Elife. 2020;9:e52511.
17. Wu F, Mo Q, Wan X, et al. NEAT1/hsa-mir-98-5p/MAPK6 axis is involved in non-small-cell lung cancer development. J Cell Biochem. 2019;120(3):2836-2846.
18. Hu C, Huang S, Wu F, et al. miR-98 inhibits cell proliferation and induces cell apoptosis by targeting MAPK6 in HUVECs. Exp Ther Med. 2018;15(3):2755-2760.
19. Lv P, Qiu X, Gu Y, et al. Long non-coding RNA SNHG6 enhances cell proliferation, migration and invasion by regulating miR-26a-5p/MAPK6 in breast cancer. Biomed Pharmacother. 2019;110:294-301.